



# Patchouli alcohol suppresses castration-resistant prostate cancer progression by inhibiting NF- $\kappa$ B signal pathways

Jian Cai, Juan Zhao, Ping Gao, Yuguo Xia

Department of Urology and Andrology, Hospital of Chengdu University of Traditional Chinese Medicine, Chengdu, China

**Contributions:** (I) Conception and design: J Cai; (II) Administrative support: Y Xia; (III) Provision of study materials or patients: J Zhao, J Cai; (IV) Collection and assembly of data: P Gao; (V) Data analysis and interpretation: J Cai, J Zhao; (VI) Manuscript writing: All authors; (VII) Final approval of manuscript: All authors.

**Correspondence to:** Jian Cai. Hospital of Chengdu University of Traditional Chinese Medicine, No. 39 Shi-er-Qiao Road, Chengdu, China. Email: caicai7811@126.com.

**Background:** There is evidence that patchouli alcohol (PA) has cytotoxic effects on human cancer cell lines, including inhibiting cell growth, migration, and invasion. However, the exact molecular mechanism of PA in human castration-resistant prostate cancer (CRPC) cells remains unclear.

**Methods:** DU145 and PC-3 cells were treated with different concentrations of PA for 48 h. Cell counting kit-8 (CCK-8), colony formation, and 5-ethynyl-2'-deoxyuridine (EdU) staining were used to detect cell proliferation. Scratch tests and transwell assays were used to detect cell migration and invasion. TdT-mediated dUTP nick-end labeling (TUNEL) staining and flow cytometry were performed to examine apoptosis and mitochondrial membrane potential. The expression of the apoptosis- and migration-related proteins and the phosphorylation of the nuclear factor kappa -B (NF- $\kappa$ B) cells were detected by Western blot. A chromatin immunoprecipitation (ChIP) analysis was conducted to examine NF- $\kappa$ B p65 binding to the myeloid cell leukemia-1 (Mcl-1) promoter. A xenograft model of nude mice was established to verify the anticancer effects of PA *in vivo*.

**Results:** PA inhibited the proliferation, migration, and invasion, and induced the apoptosis of the DU145 and PC-3 cells in a concentration-dependent manner, and was accompanied by mitochondrial membrane potential depolarization, the upregulation of cleaved caspase-3, cleaved poly ADP-ribose polymerase (PARP) and Bcl-2-associated X protein (Bax), and the downregulation of B-cell lymphoma-2 (Bcl-2), Ki67, and Mcl-1. In relation to the mechanism, PA significantly downregulated the phosphorylation of inhibitor of NF- $\kappa$ B  $\alpha$  (I $\kappa$ B $\alpha$ ) and p65 and the expression of matrix metalloprotein (MMP)-2, MMP-7, MMP-9, and vascular endothelial growth factor (VEGF). PA prevented p65 binding to the Mcl-1 promoter by inactivating NF- $\kappa$ B p65, downregulated the transcription of Mcl-1, and the silencing of p65 increased the sensitivity of the CRPC cells to PA-induced apoptosis. The overexpression of Mcl-1 significantly reversed the PA-induced apoptosis of the CRPC cells. Additionally, consistent with our *in-vitro* study, PA inhibited tumor growth in the mouse xenograft model.

**Conclusions:** We found that PA inhibits the growth, migration, and invasion of CRPC cells *in vitro* and *in vivo* by inducing an apoptosis mechanism and inhibiting NF- $\kappa$ B activity. Our findings may provide therapeutic targets for this malignant tumor.

**Keywords:** Patchouli alcohol (PA); castration-resistant prostate cancer (CRPC); nuclear factor kappa-B (NF- $\kappa$ B); Mcl-1; apoptosis

Submitted Mar 17, 2022. Accepted for publication Apr 08, 2022.

doi: 10.21037/tau-22-220

View this article at: <https://dx.doi.org/10.21037/tau-22-220>

## Introduction

Prostate cancer (PCa) is the 5th most common malignant tumor in the world, and the mortality rate of PCa in men is 2nd only to that of lung cancer (1). In terms of genitourinary tumors, PCa is the most common malignancy in men and is even more common than bladder cancer (1). PCa is an androgen-dependent tumor (2). Androgen deprivation therapy (ADT), the mainstay of treatment for advanced PCa, despite an initial response to ADT, subsequently induces resistance, which eventually leads to relapse and the development of a more aggressive disease called castration-resistant prostate cancer (CRPC) (3-5). Thus, the prevention and treatment of CRPC is the focus of current PCa research (2,6). At present, there are many chemotherapeutic drugs, hormone inhibitors, and tumor vaccines for the treatment of CRPC (6-8); however, these chemical synthetic drugs have side effects after treatment. Thus, finding low-toxic drugs that can be used for the treatment of CRPC is of great significance to the clinical treatment of CRPC.

Patchouli alcohol (PA) is a tricyclic sesquiterpene isolated from *pogostemon cablin*, labiatae. Its molecular formula is  $C_{15}H_{26}O$  and it has a molecular weight of 222.37. Its chemical structure is shown in *Figure 1A*. It has a variety of therapeutic effects; for example, it is anti-inflammatory (9), anti-ulcer (10), anti-bacterial (11), and protects intestinal epithelial cell fluidity (12). Recently, some studies have shown the anticancer activity and potential mechanism of PA. For example, research has shown that PA inhibited cell proliferation and induced apoptosis in 2 human colorectal cancer cell lines (i.e., HCT116, and SW480) in a concentration-dependent manner (9). Lu *et al.* showed that PA induced apoptosis and cell cycle arrest in A549 cancer cells *in vitro* and *in vivo* by blocking phosphorylation of the EGFR pathway and activating the JNK pathway (13). Additionally, PA significantly inhibited the proliferation of gastric cancer cells, inhibited the migration, and invasion activities in a dose-dependent manner, and induced apoptosis (14). However, very little research has been conducted on the anti-cancer ability of PA on human PCa. In this study, we found that PA inhibited the growth of DU145 and PC-3 cells *in vitro* and induced apoptosis. Further experiments on the molecular mechanism showed that PA inhibited the phosphorylation of nuclear factor kappa-B (NF- $\kappa$ B), thereby downregulating the expression of the anti-apoptotic key gene myeloid cell leukemia-1 (Mcl-1), which may be the reason for the anti-cancer

activity of PA. Myeloid leukemia 1 (MCL-1) is an anti-apoptotic protein of the BCL-2 family, which can prevent apoptosis by combining apoptotic Bcl-2 protein (15). MCL-1 is expressed in many tumor types and is closely related to tumor, prognosis and drug resistance (15). The core effect of MCL-1 in the adjustment of mitochondrial apoptosis makes it an attractive target of cancer treatment. Our research suggests that PA may be a potential compound for the treatment of CRPC in clinical practice, and provides new reference information for the development and application of PA. We present the following article in accordance with the ARRIVE reporting checklist (available at <https://tau.amegroups.com/article/view/10.21037/tau-22-220/rc>).

## Methods

### Materials

Fetal bovine serum (FBS), pancreatin, Roswell Park Memorial Institute Medium (RPMI)-1640 medium, phosphate buffered saline (PBS), penicillin, and streptomycin were supplied from Gibco (Carlsbad, USA). The human CRPC cell lines DU145 and PC-3 were purchased from the American Type Culture Collection (ATCC, USA). PA standard (purity >98%) was purchased from the National Institute for Pharmaceutical and Biological Products (Beijing, China). The terminal deoxynucleotidyl transferase (TdT)-mediated dUTP nick-end labeling (TUNEL) Apo-Green kit was provided by Roche (Basel, Switzerland). The cell counting kit-8 (CCK-8), annexin V-fluorescein isothiocyanate (FITC), propidium iodide (PI), caspase-3 activity assay kit, colorimetric TUNEL apoptosis assay kit, radio immunoprecipitation assay (RIPA) cell lysate buffer, BeyoECL Plus, bicinchoninic acid (BCA) protein assay kit, dimethyl sulfoxide (DMSO), and 4', 6-diamino-2-phenylindole (DAPI) were purchased from Biyuntian Institute of Biotechnology (Haimen, China). Matrigel was purchased from BD (USA). The JC-1 mitochondrial membrane potential assay kit was purchased from AAT Bioquest (CA, USA). The Cell-Light EdU Apollo 488 *in-vitro* kit was purchased from RiboBio (Guangzhou, China). The desired primary antibodies and the horseradish peroxidase (HRP)-labeled anti-mouse/anti-rabbit secondary antibodies were provided by Cell Signaling Technology (Beverly, USA). Trizol reagent and Lipofectamine 2000 were purchased from Invitgen (USA). Reverse transcription

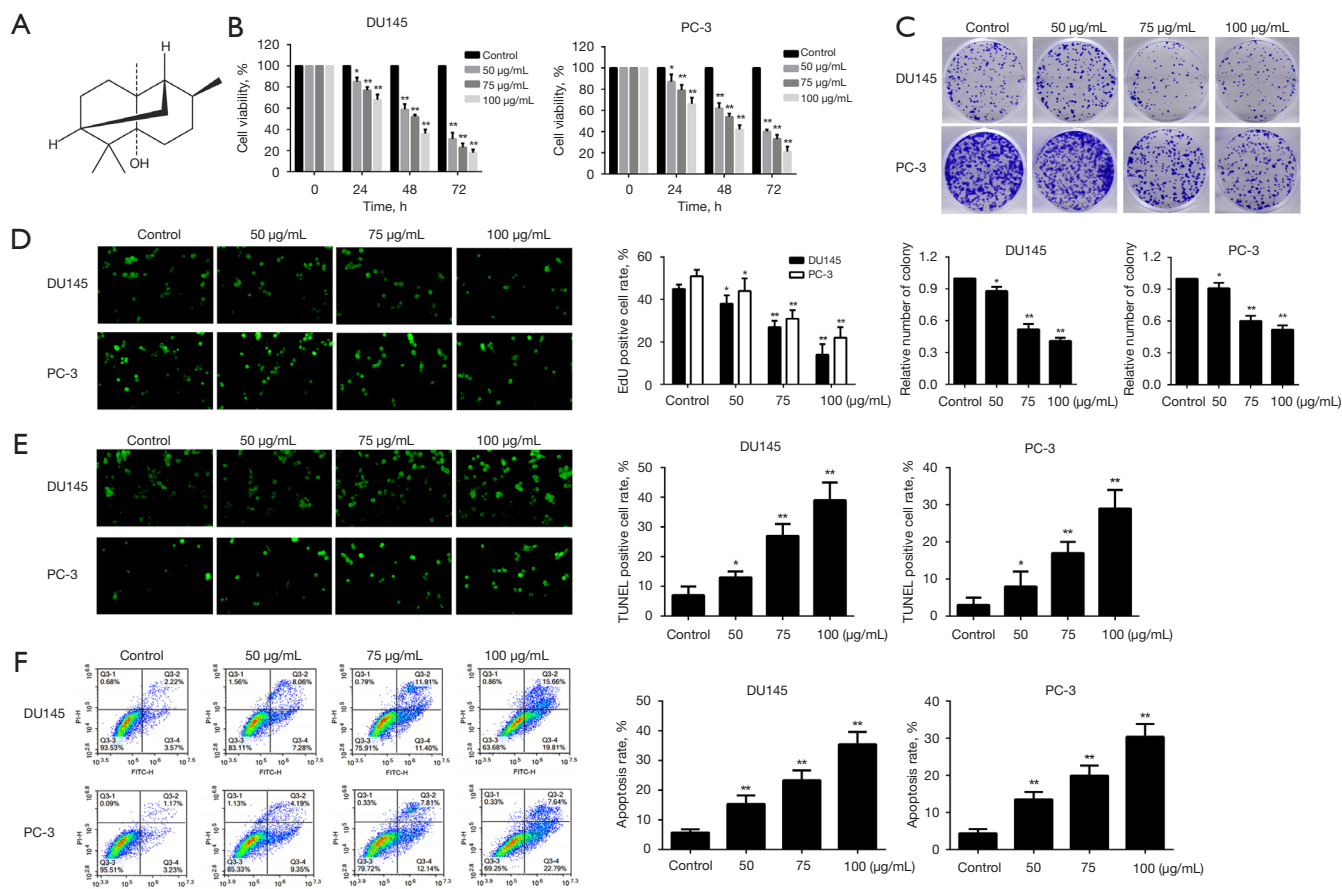


**Figure 1** PA inhibits the proliferation and induces the apoptosis of human CRPC cells. (A) The chemical structure of PA. (B) After the DU145 and PC-3 cells were treated with different concentrations of PA for 24 h, 48 h, and 72 h, CCK-8 assays were used to detect cell viability. (C) After the DU145 and PC-3 cells were treated with 0, 50, 75, and 100  $\mu\text{g/mL}$  for 14 days, cell proliferation was detected by crystal violet staining ( $\times 100$ ). (D) After the DU145 and PC-3 cells were treated with 50, 75, and 100  $\mu\text{g/mL}$  for 48 h, cell proliferation was observed by EdU fluorescence staining ( $\times 100$ ). (E) After the DU145 and PC-3 cells were treated with 0, 50, 75, and 100  $\mu\text{g/mL}$  PA for 48 h, the apoptosis levels were detected using TUNEL method ( $\times 100$ ). (F) After the DU145 and PC-3 cells were treated with 0, 50, 75, and 100  $\mu\text{g/mL}$  for 48 h, the apoptosis rates were detected by Annexin V-FITC/PI staining. The data are expressed as the mean  $\pm$  SD for the 3 independent experiments. Compared to the control group, \*,  $P < 0.05$ ; \*\*,  $P < 0.01$ . CRPC, castration-resistant prostate cancer; PA, patchouli alcohol; CCK-8, cell counting kit-8; EdU, 5-ethynyl-2'-deoxyuridine; TUNEL, TdT-mediated dUTP nick-end labeling; PI, propidium iodide; SD, standard deviation.

kits were purchased from Promega (Madison, WI, USA). The SYBR Green Polymerase Chain Reaction (PCR) Master Mix was purchased from Takara (Dalian, China). The chromatin immunoprecipitation (ChIP) analysis kit was purchased from Upstate Biotechnology (Lake Placid, NY, USA). Any of the other chemical reagents not mentioned above were analytical grade.

#### Cell cultures and PA treatments

The cells were grown in RPMI-1640 medium containing 10% FBS and a 1% antibiotic mixture (100  $\mu\text{g/mL}$  of streptomycin, and 100 U/mL of penicillin) and incubated at 37  $^{\circ}\text{C}$  with 5% carbon dioxide ( $\text{CO}_2$ ). The PA standard was dissolved in DMSO for further experiments. In the PA treatment group, the required hours for the 2 cell lines to

be treated with different concentrations of PA. The control group received the same volume of DMSO under the same conditions.

### *CCK-8 assays*

The DU145 and PC-3 cells were seeded in 96-well plates with  $5 \times 10^3$  cells/well. After overnight culturing, the cells were further cultured in the drug-containing medium with PA concentrations of 0, 50, 75, or 100  $\mu\text{g}/\text{mL}$ , with 3 replicate wells in each group. After incubation for 24, 48, and 72 h, 10  $\mu\text{L}$  of CCK-8 solution was added, and the cells were incubated at 37 °C for 2 h. Absorbance was detected at 450 nm using a Benchmark microplate reader (Dali, California, USA). The cell survival rate (%) was calculated as follows: [(experimental group-blank group)/(control group-blank group)]  $\times 100\%$ .

### *Colony formation assays*

The cells were seeded in 6-well cell culture plates with 200 cells/well and incubated for 24 h. After 48 h of treatment with different concentrations of PA (0, 50, 75, or 100  $\mu\text{g}/\text{mL}$ ) in each well, the cell culture medium was removed, and the cells were cultured in a new medium at 37 °C with 5%  $\text{CO}_2$  for 2 weeks. The clones were fixed in 4% paraformaldehyde for 20 min, and stained with 0.1% crystal violet solution at room temperature for 15 min. The colonies were counted under the light microscope, and those with  $\geq 25$  cells were classified as colonies. The experiment was repeated 3 times.

### *EdU staining assays*

A total of  $5 \times 10^4$  cells/well were seeded in 24-well plates. After 12 h of culturing, different concentrations of PA (0, 50, 75, or 100  $\mu\text{g}/\text{mL}$ ) were incubated for 48 h, and EdU working solution (10  $\mu\text{M}$ ) was then added to each well. After 2 h of incubation, the cells were fixed with 4% paraformaldehyde for 30 min, washed 3 times with immunostaining detergent, and infiltrated with 0.1% TritonX-100 for 15 min. After washing 3 times with immunostaining lotion, the nuclei were stained with DAPI for 10 min. Anti-fluorescence quenching agent was added to prevent cell fluorescence quenching. Finally, a fluorescence microscope ( $\times 100$  magnification; Olympus, Tokyo, Japan) was used to observe the staining.

### *Wound-healing tests*

The DU145 and PC-3 cells were inoculated into 6 well plates. After the cells were fully integrated, the monolayer was wiped with a 10- $\mu\text{L}$  suction nozzle, and the cells were washed with PBS to remove any cell debris. Next, PA at different concentrations (0, 50, 75, or 100  $\mu\text{g}/\text{mL}$ ) was used to treat the cells for 48 h. At 0 and 48 h after scratching, the scratches were imaged with a 10-time objective lens, and the cell migration rates were calculated.

### *Transwell assays*

The membrane of each upper room was wrapped with Matrigel (100  $\mu\text{g}/\text{cm}^2$ ), and then incubated overnight at 37 °C to gel. The DU145 and PC-3 cells were incubated with different concentrations of PA (0, 50, 75, or 100  $\mu\text{g}/\text{mL}$ ) for 48 h, and then suspended in serum-free medium and inoculated into the upper transwell chamber. FBS (10%) was added to the lower chamber as a chemical inducer. After 48 h of culturing in the incubator, the cells were washed 3 times with PBS, fixed with 4% paraformaldehyde for 2 min at room temperature, permuted with 100% methanol for 20 min, and then stained with crystal violet solution for 15 min. The cells that adhered to the upper surface of the chamber were carefully removed by cotton swabs, and the cells on the bottom surface of the membrane were imaged. Cells were counted from 5-field randomly selected under the optical microscope (Leica, Germany). The experiment was repeated 3 times.

### *TUNEL assays*

The DU145 and PC-3 cells were seeded in 24-well plates with  $3 \times 10^5$  cells per well for 24 h. On the next day, PA (0, 50, 75, or 100  $\mu\text{g}/\text{mL}$ ) was used to treat the cells for 48 h, and the cells were then fixed with 4% methanol-free formalin and kept at 4 °C for 25 min, after which they were washed with PBS for 5 min. Next, the cells were digested with lysis buffer (1% Triton X-100 in 1% sodium citrate) for 5 min, and then treated with 50  $\mu\text{L}$  of terminal deoxyribonucleotidyl transferase (TdT) enzyme buffer. Subsequently, the labeled strand breaks were confirmed by the attachment of fluorescein isothiocyanate-5-dUTP. Finally, each well was stained with DAPI and observed using a fluorescence microscope (an IX-73 inverted microscope, Olympus). For the tumor sections, after dewaxing

and hydration in accordance with the manufacturer's instructions, a TUNEL apoptosis detection kit was used to detect the apoptosis of the tumor tissues, and the results were observed under a fluorescence microscope.

#### *Investigation of apoptosis through flow cytometry*

The DU145 and PC-3 cells were collected and washed with PBS. Annexin V-FITC was used to stain the cells in the dark at room temperature for 30 min, and the cells were then incubated with PI. The stained cells were analyzed by Accuri C6 flow cytometry (Accuri Inc., Ann Arbor, MI, USA). Annexin V-FITC(-)/PI(-) (left-lower quadrant) indicates normal cells, Annexin V-FITC(-)/PI(+) (left-upper quadrant) indicates necrotic cells, Annexin V-FITC(+)/PI(-) (right-lower quadrant) indicates early apoptotic cells, Annexin V-FITC (+)/PI(+) (right upper quadrant) indicates late apoptotic cells.

#### *Mitochondrial membrane potential*

The PC-3 and DU145 cells were seeded in 6-well plates ( $2 \times 10^5$ /well) and treated with PA (0, 50, 75, or 100  $\mu\text{g}/\text{mL}$ ) for 48 h. The cells were collected in brown Eppendorf tubes and washed twice with PBS. Next, 1  $\mu\text{L}$  of JC-1 was dissolved in 500  $\mu\text{L}$  1 $\times$  culture buffer to produce the JC-1 working solution, and the liquid was then added to the suspended cells. After being incubated for 15 min, the cells were washed twice with 1 $\times$  incubation buffer. Accuri C6 flow cytometry (Accuri Inc., Ann Arbor, MI, USA) was used to determine the relative amount of mitochondrial JC-1 monomer or aggregate dual emission.

#### *Western blotting*

The DU145 and PC-3 cells were lysed with RIPA cell lysate containing protease inhibitors. The lysates were centrifuged at 4  $^{\circ}\text{C}$  (14,300  $\times g$ ) for 15 min and the supernatant was collected. A BCA protein assay kit was used to measure the protein concentration. For protein imprinting, the same amount of protein (40  $\mu\text{g}$ ) from each sample was loaded onto 12% sodium dodecyl sulfate-polyacrylamide gel electrophoresis gel, and the separated protein was electro-imprinted onto the polyvinylidene fluoride membranes. Next, the membrane was sealed with 5% skim milk for 1 h at room temperature, washed with PBS, and incubated with primary antibody overnight at 4  $^{\circ}\text{C}$ . The cells were washed with Tris buffered saline with Tween was washed 3 times,

5 min each time, and incubated with HRP-labeled secondary antibody for 1 h. A chemiluminescence imaging system (Clinx, Shanghai, China) was used to obtain strip images.

#### *Caspases 3 activity assays*

The PC-3 and DU145 cells were treated with PA (0, 50, 75, or 100  $\mu\text{g}/\text{mL}$ ) for 48 h, after which cell lysate was added. The cells were centrifuged at 3,000 r/min at 4  $^{\circ}\text{C}$  for 15 min to detect the protein concentration. The supernatant was then transferred to a pre-cooled centrifuge tube and placed on ice for standby. In accordance with the kit's instructions, a cysteine aspartate protease 3 activity kit was used to determine the activity of cysteine aspartate protease 3. The release of p-nitroaniline was measured by a microplate reader at 405 nm. Caspase activity was expressed as the ratio of the PA treated cells to the control cells.

#### *Cell transfections*

In the CRPC cells, p65 was silenced by p65 small-inhibitory ribonucleic acid (siRNA). The P65 siRNA was synthesized by GenePharma (Shanghai, China). The cells were seeded in 6-well plates and incubated for 24 h. Next, p65 siRNA or scrambled siRNA was transiently transfected with Lipofectamine 2000 reagent in accordance with the manufacturer's instructions. After 48 h of transfection, the cells were collected for the Western blot analysis and subsequent experiments. The full-length complementary deoxyribonucleic acid (cDNA) of the human *Mcl-1* gene (NM\_021960) in the PCMV6 vector was purchased from Origene (Rockville, Maryland, USA). The empty vector or Mcl-1 expression plasmid was transfected into the cells with Lipofectamine 2000 for 48 h to collect cells for the Western blot analysis and verification and the subsequent experiments.

#### *Real-time quantitative reverse transcription (qRT)-PCR assay*

Total RNA was extracted from the 2 cell lines by Trizol reagent and reverse transcribed into cDNA using a reverse transcription kit. The PCR was amplified using the SYBR Green PCR Master Mix and the following PCR primers (16): Mcl-1 forward: 5'-GCCAAGGACACAAAGCCAAT-3' and reverse: 5'-AACTCAAACCCATCCCA-3';  $\beta$ -actin forward: 5'GGGACCGTAGCGCCTGCGACT-3', and



reverse: 5'-TCGTCCATGGCCCGCTGACTC-3'. The Mcl-1 mRNA expression level was calculated using the comparative cycle threshold (Ct) method ( $2^{-\Delta\Delta C_t}$ ) and by normalizing the target messenger RNA (mRNA) Ct values to those for  $\beta$ -actin, and all the samples were analyzed in triplicate.

### ChIP analysis

A ChIP analysis kit was used for the ChIP experiment, as described in (16). After immunoprecipitation with anti-NF- $\kappa$ B p65 (1:100 dilution) or control immunoglobulin G, the antibody-binding complex was treated with ribonuclease A/proteinase K. The ChIP DNA (17) was purified and amplified with Mcl-1 promoter specific primers: forward: 5'-CACTTCTCACTTCCGCTTCC-3' and reverse: 5'-TTCTCCGTAGCCAAAAGTCG-3'. The PCR products were analyzed by 1.2% agarose gel electrophoresis and stained with ethyl bromide. The chromatin samples treated by ultrasound were used as the input control.

### Animal experiments

BALB/c nude mice (aged 4–6 weeks and weighing 18–20 g) were purchased from Beijing Vital River Laboratory Animal Technology Co., Ltd. (China). Each mouse was intraperitoneally injected with  $5 \times 10^6$  PC-3 cells/100  $\mu$ L. After tumor growth, the mice were randomly divided into the following 2 groups (6 per group): (I) the control group; and (II) the PA group. The PA group was intraperitoneally injected with 100  $\mu$ L of PA (15 mg/kg) dissolved in 5% DMSO solution, the used dose according to Lu *et al.* (13). The nude mice were intraperitoneally injected with the same volume containing 5% DMSO once every 3 days. All the tumors were measured every 3 days. The tumor size was calculated as follows: volume = (length  $\times$  width<sup>2</sup>)/2. After 30 days, the tumor-bearing mice were sacrificed, and the primary solid tumors were removed and weighed. The tumors were fixed overnight in 4% paraformaldehyde for the immunohistochemical analysis and TUNEL detection. The main organs, including the heart, liver, spleen, kidneys and lungs, were collected for histological detection by routine hematoxylin and eosin (H&E) staining. Animal experiments were performed under a project license (No. 2015-BL002) granted by ethics board of Hospital of Chengdu University of Traditional Chinese Medicine, in compliance with the guidelines of the

National Institutes of Health (NIH) for the care and use of animals (18). A protocol was prepared before the study without registration.

### Immunohistochemistry

The tissue sections were baked at 60 °C for 10 min, and then dewaxed in xylene solution 3 times (10 min each time), and rehydrated with gradient ethanol (100%, 95%, 85%, 75%, and 50%). The catalase was removed with 0.3% hydrogen peroxide, and the antigen was recovered by heating with pH 6.0 citric acid buffer. After blocking with 10% goat serum at room temperature for 1 h, Ki67, p-p65, cleaved caspase-3, Mcl-1, and MMP-2 were detected by rabbit polyclonal antibody. After washing with PBS for 3 times, the tissue sections were incubated with biotinylated anti-rabbit secondary antibody, or HRP-conjugated streptavidin. Next, the slices were incubated with diaminobenzidine solution and stained with hematoxylin. Finally, the slices were observed and photographed under fluorescence microscope (using an IX-73 inverted microscope, Olympus).

### Statistical analysis

All the data are expressed as the mean  $\pm$  standard deviation (mean  $\pm$  SD). The statistical data were analyzed by the student's *t*-test or a one-way analysis of variance (GraphPad Prism 7 Software). A *P* value <0.05 indicated that the difference was statistically significant.

## Results

### *PA inhibits the proliferation and induces the apoptosis of human CRPC cells in vitro*

To analyze the effect of PA on the proliferation of human CRPC cells, CCK-8 was employed to detect the cell survival rates of the DU145 and PC-3 cells treated with the PA concentration gradient (0, 50, 75, or 100  $\mu$ g/mL) at different times (24, 48, and 72 h). PA effectively inhibited the activity of the 2 CRPC cell lines in a concentration- and time-dependent manner (see *Figure 1B*). The IC<sub>50</sub> values of the DU145 and PC-3 cells at 48 h were 70.08 and 79.38  $\mu$ g/mL, respectively. Thus, in the subsequent experiments, the cells were treated with PA for 48 h. Next, the results of the colony formation experiment showed that PA significantly reduced the colony formation of the DU145 and PC-3 cells after 14 days of continuous

treatment (see *Figure 1C*) in a concentration-dependent manner. Additionally, EdU fluorescence staining was further used to visually verify the inhibitory effects of PA on cell proliferation. Compared to the control group, the number of EdU positive cells in the PA treatment group was significantly decreased (see *Figure 1D*). To investigate whether the decrease of cell viability was related to the apoptosis induction of DU145 and PC-3 cells, TUNEL staining was used to detect cell apoptosis. As *Figure 1E* shows, the green fluorescence intensity of the PA 50, 75, and 100  $\mu\text{g/mL}$  groups was significantly enhanced compared to that of the control group, and the degree of apoptosis was related to the drug concentration. Next, Annexin V-FITC/PI staining flow cytometry was used to further analyze the apoptosis rate of the DU145 and PC-3 cells. As *Figure 1F* shows, with the increase of PA concentration, the apoptosis rate (early and late) was significantly increased in a concentration-dependent manner.

#### ***PA suppresses the migration of CRPC cells in vitro***

We used wound-healing and transwell assays to determine the effects of PA on DU145 and PC-3 cell metastasis. As *Figure 2A,2B* show, the healing rate of the scratches decreased significantly after PA treatment. The transwell analysis showed that PA treatment significantly reduced the number of invasive cells in a dose-dependent manner (see *Figure 2C,2D*). Additionally, as *Figure 2E* shows, the Western blot analysis showed that MMP-2, MMP-7, MMP-9, vascular endothelial growth factor (VEGF), and N-cadherin protein expressions were significantly downregulated in the DU145 and PC-3 cells, while the expression of E-cadherin was significantly upregulated, suggesting that PA inhibits the movement of human CRPC cells.

#### ***PA induces the apoptosis of CRPC cells through the mitochondrial apoptotic pathway***

Next, we examined whether the PA-induced apoptosis involved mitochondrial dysfunction. First, JC-1 was used to detect the change of mitochondrial membrane potential. After 48 h of PA treatment, the flow cytometry analysis showed that the disintegration of mitochondrial membrane potential occurred in a concentration-dependent manner (see *Figure 3A*), suggesting that PA induced mitochondrial membrane depolarization. The Western blot analysis showed that PA inhibited the expression of anti-apoptotic

protein Bcl-2 and enhanced the expression of pro-apoptotic protein Bax, resulting in a significant increase in the ratio of Bax/Bcl-2. The cleavage levels of PARP and the caspase-3 and caspase-3 activity in the cells increased in a concentration-dependent manner (see *Figure 3B,3C*). Additionally, the caspase inhibitor (10  $\mu\text{M}$  of Z-VAD-FMK) pretreatment of the DU145 and PC-3 cells for 3 h significantly promoted cell survival and inhibited cell apoptosis compared to the single PA treatment (see *Figure 3D*). Thus, PA induced CRPC cell apoptosis via the mitochondrial cascade pathway.

#### ***PA induces the apoptosis of human CRPC cells by inhibiting NF- $\kappa$ B and downregulating Mcl-1***

As an important transcriptional regulator, NF- $\kappa$ B p65 protein is involved in the occurrence and development of many cancers. More importantly, the continuous activation of the NF- $\kappa$ B signaling pathway plays a key role in the progression of PCa to castrate-resistant and metastatic cancer. Thus, we evaluated whether the anti-tumor effect of PA on the DU145 and PC-3 cells was closely related to the inhibition of the NF- $\kappa$ B signaling pathway. As *Figure 4A* shows, the Western blot data showed that the ratio of phosphorylated inhibitor of NF- $\kappa$ B  $\alpha$  (I $\kappa$ B $\alpha$ ) (Ser32/36) and phosphorylated p65 (Ser536) decreased in a concentration-dependent manner after PA treatment, suggesting that the role of PA in inhibiting the NF- $\kappa$ B signaling pathway may be related to its inhibiting the degradation of I $\kappa$ B $\alpha$  and p65 in DU145 and PC-3 cells.

NF- $\kappa$ B is an important transcription factor of the apoptosis key regulatory gene Mcl-1, and we found that the Mcl-1 protein was downregulated in PA concentration-dependent manner, and Mcl-1 mRNA abundance was also reduced by PA treatment (see *Figure 4A,4B*), which is consistent with the change of the NF- $\kappa$ B pathway. The ChIP analysis showed that PA treatment reduced the binding of NF- $\kappa$ B p65 to the Mcl-1 promoter (see *Figure 4C*). This confirmed that PA treatment inhibited Mcl-1 expression through NF- $\kappa$ B.

To confirm whether the PA-induced apoptosis of the CRPC cells was related to the inhibition of the NF- $\kappa$ B signaling pathway, p65 siRNA and scrambled siRNA were transfected into the DU145 and PC-3 cells, respectively, which were then treated with PA (75  $\mu\text{g/mL}$ ) for 48 h. As *Figure 4D* shows, the expression level of p65 in the cells transfected with p65 siRNA was significantly lower than that in the cells transfected with scrambled siRNA.

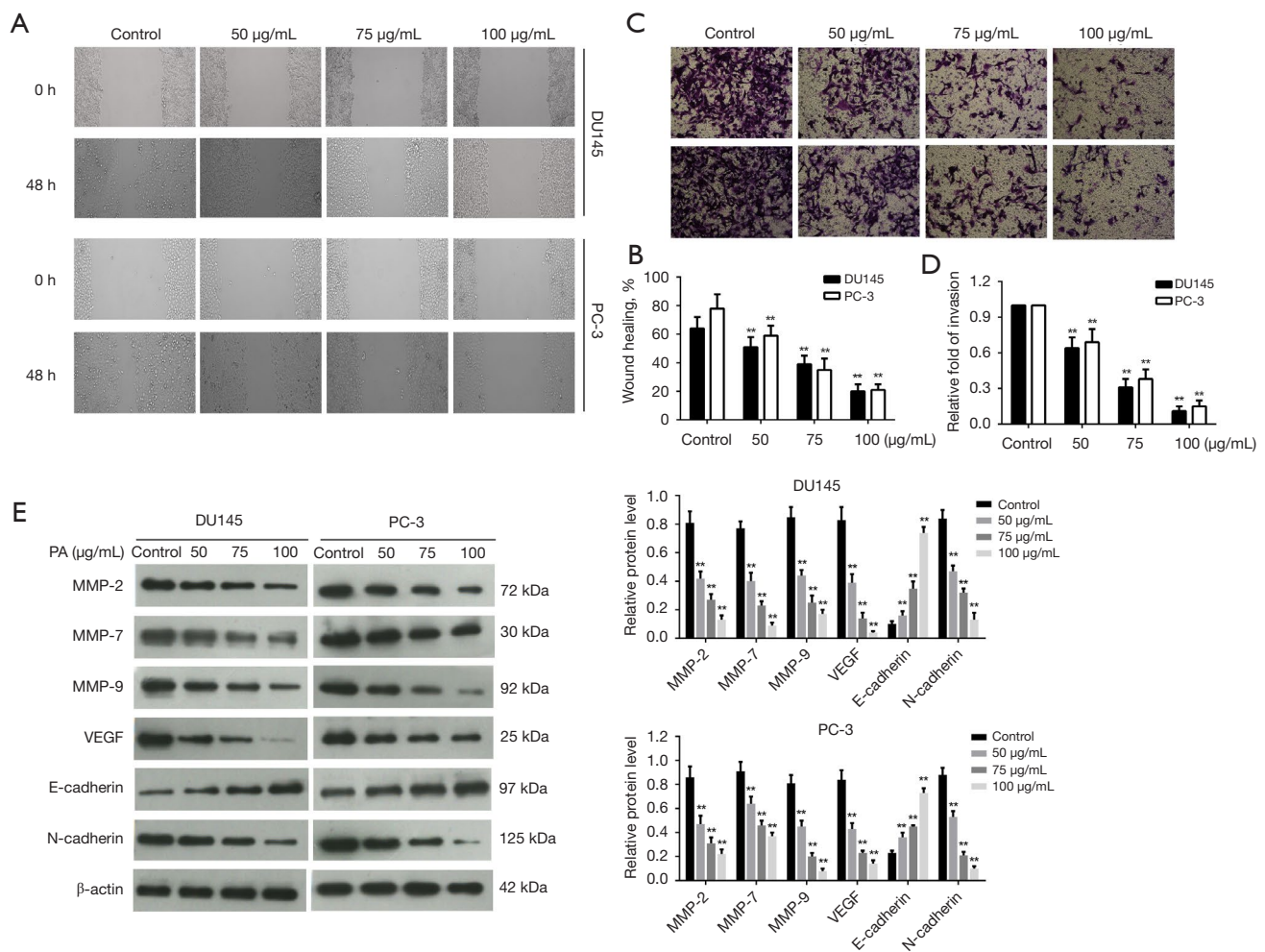


**Figure 2** PA suppresses the migration, and invasion of human CRPC cells. After treatment with 0, 50, 75, and 100 µg/mL for 48 h, the DU145 and PC-3 cells were subjected to (A) images of monolayers were captured under an optical light microscope (×100) following wounding 48 h and (B) quantification of cell migration in (A). (C) transwell tests (crystal violet staining, ×200) and (D) quantification of cell invasion in (C). (E) The relative expression of MMP-2, MMP-7, MMP-9, VEGF, E-cadherin, N-cadherin, and β-actin protein in the DU145 and PC-3 cells treated with 0, 50, 75, and 100 µg/mL for 48 h. The data are expressed as the mean ± SD for the 3 independent experiments. Compared to the control group, \*\*, P<0.01. PA, patchouli alcohol; CRPC, castration-resistant prostate cancer; MMP, matrix metalloprotein; VEGF, vascular endothelial growth factor; SD, standard deviation.

Additionally, the study results showed that the cell survival rate was significantly decreased (see *Figure 4E*), and the cell mortality in p65 siRNA + PA group was significantly higher than that of the cells transfected with scrambled siRNA + PA group (see *Figure 4F*).

***Mcl-1 overexpression protects human CRPC cells from PA-induced apoptosis***

Next, we examined whether the expression of the Mcl-

1 rescued PA-induced DU145 and PC-3 cell apoptosis. The Western blot analysis confirmed that the expression of Mcl-1 in the DU145 and PC-3 cells increased after the transfection of the Mcl-1 expression plasmid (see *Figure 5A,5B*). Compared to the empty vector transfected cells, the IC50 values of the DU145 and PC-3 cells in the Mcl-1 overexpression group were significantly increased (see *Figure 5C*). Additionally, the overexpression of Mcl-1 significantly reduced the apoptosis of the DU145 and PC-3 cells induced by PA (75 µg/mL) (see *Figure 5D,5E*). These



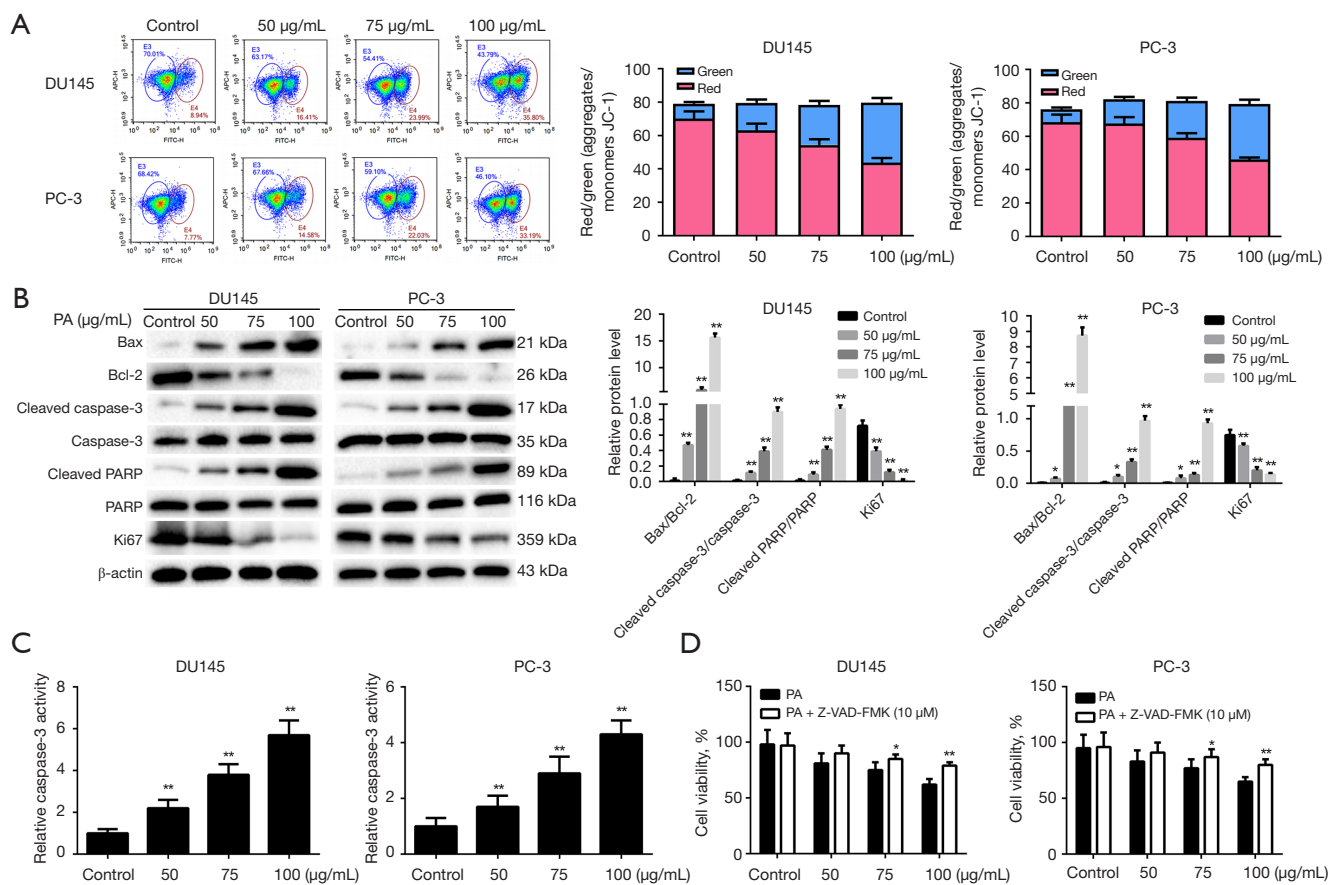


**Figure 3** PA induces the apoptosis of human CRPC cells via the mitochondrial apoptosis pathway. (A) After the DU145 and PC-3 cells were treated with PA (0, 50, 75, and 100 µg/mL, respectively) for 48 h, mitochondrial membrane potential was determined by JC-1 staining flow cytometry. (B) After the DU145 and PC-3 cells were treated with PA (0, 50, 75, and 100 µg/mL, respectively) for 48 h, the protein expressions of Bax, Bcl-2, Cleaved caspase-3, caspase-3, Cleaved PARP, PARP, Ki67, and β-actin were detected by Western blot. (C) Measurement of relative caspase-3 activity in the DU145 and PC-3 cells treated with PA 0, 50, 75, and 100 µg/mL for 48 h. The results are expressed as the mean ± SD. Compared to the control group, \*,  $P < 0.05$ ; \*\*,  $P < 0.01$ . (D) The treatment group was pretreated with a caspase inhibitor (10 µM of Z-VAD-FMK) for 3 h and incubated with PA (0, 50, 75, and 100 µg/mL, respectively) for 48 h. CCK-8 was used to detect cell viability. The results are expressed as the mean ± SD, and compared to the corresponding group, \*,  $P < 0.05$ ; \*\*,  $P < 0.01$ . PA, patchouli alcohol; CRPC, castration-resistant prostate cancer; PARP, poly ADP-ribose polymerase; SD, standard deviation; Z-VAD-FMK, Z-VAD(OMe)-FMK, pan caspase inhibitor; CCK-8, cell counting kit-8.

results showed that Mcl-1 played a key role in PA-induced apoptosis.

### PA inhibits tumor growth in vivo

To verify the *in-vivo* inhibitory effect and molecular mechanism of PA on PCa, the PC-3 cells were inoculated subcutaneously in the nude mice to form ectopic tumors *in vivo*. Compared to the control group, the tumor volume and weight were significantly decreased under the

PA intervention (see *Figure 6A-6C*), indicating that PA significantly slowed tumor growth. The histopathological data of the main organs (heart, liver, spleen, lungs, and kidneys) showed that PA had no obvious side effects (see *Figure 6D*). Notably, the H&E staining of the testis and epididymis of the nude mice showed that PA had no significant toxicity effect on the testis and epididymis (see *Figure 6D*). Thus, PA inhibited PCa but had no obvious reproductive toxicity. The results of the immunohistochemical analysis showed that the PA

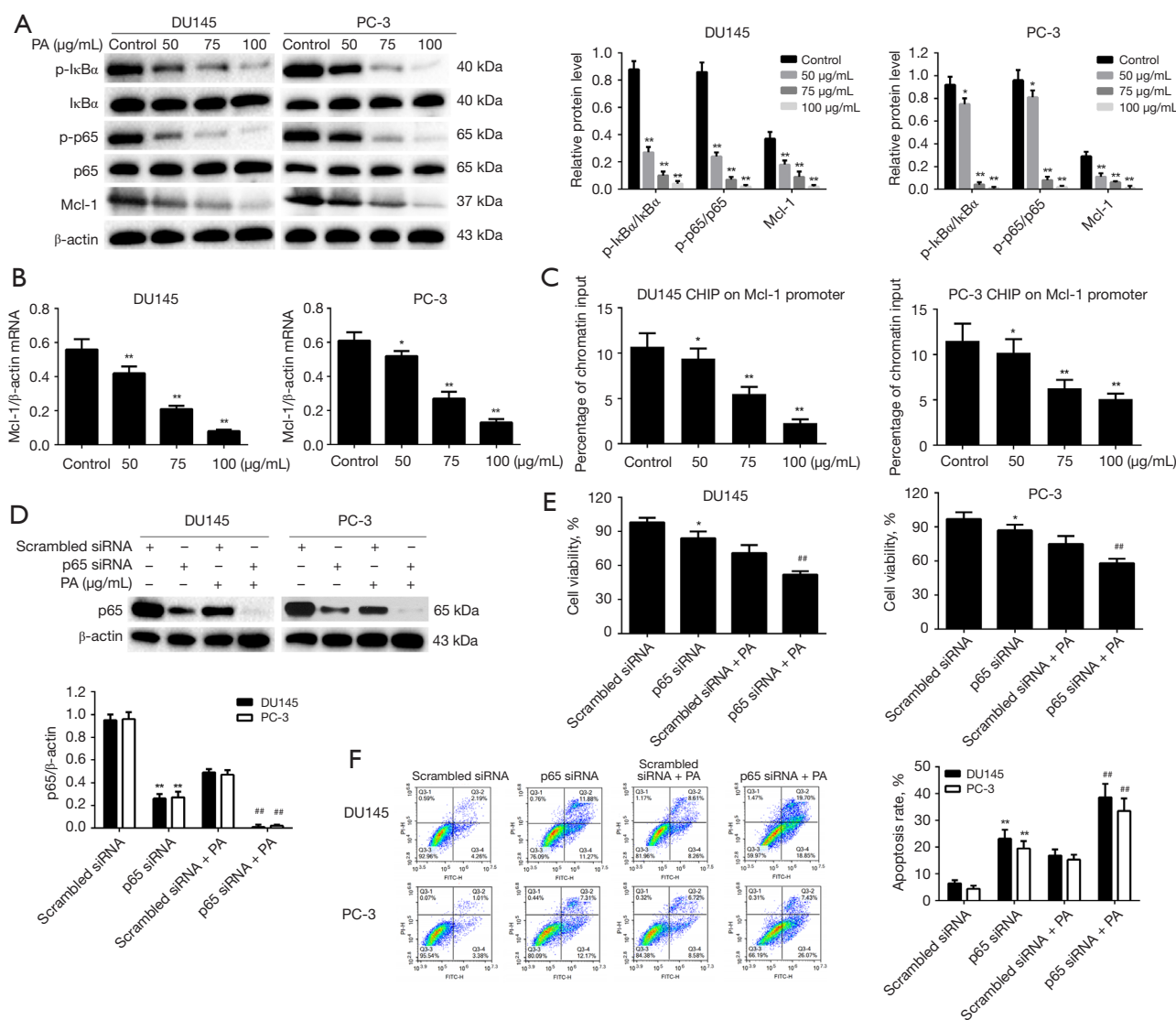


**Figure 4** PA mediates the apoptosis of CRPC cells by inhibiting NF-κB/Mcl-1. (A) After the DU145 and PC-3 cells were treated with 0, 50, 75, and 100 μg/mL PA for 48 h, the expressions of p-IκBα (Ser32/36), IκBα, p-p65 (Ser536), p65, Mcl-1, and β-actin were detected by Western blot. (B) qRT-PCR analysis of the Mcl-1 transcription levels of the DU145 and PC-3 cells. (C) ChIP analysis of the DU145 and PC-3 cells. The results are expressed as the mean ± SD. Compared to the control group, \*, P<0.05; \*\*, P<0.01. The DU145 and PC-3 cells were transfected with p65 siRNA or scrambled siRNA, and then treated with PA75 μg/mL for 48 h. (D) The expression of p65 protein was detected by Western blot. “+” indicates treated; “-” indicates that the cells are not treated. (E) Cell viability was measured by the CCK-8 method. (F) Apoptosis was detected by flow cytometry. The results are expressed as the mean ± SD. Compared to the corresponding group, \*, P<0.05; \*\*, P<0.01; ###, P<0.01. PA, patchouli alcohol; CRPC, castration-resistant prostate cancer; NF-κB, nuclear factor kappa-light-chain-enhancer of activated B; qRT-PCR, quantitative reverse transcription PCR; ChIP, chromatin immunoprecipitation; SD, standard deviation; CCK-8, cell counting kit-8.

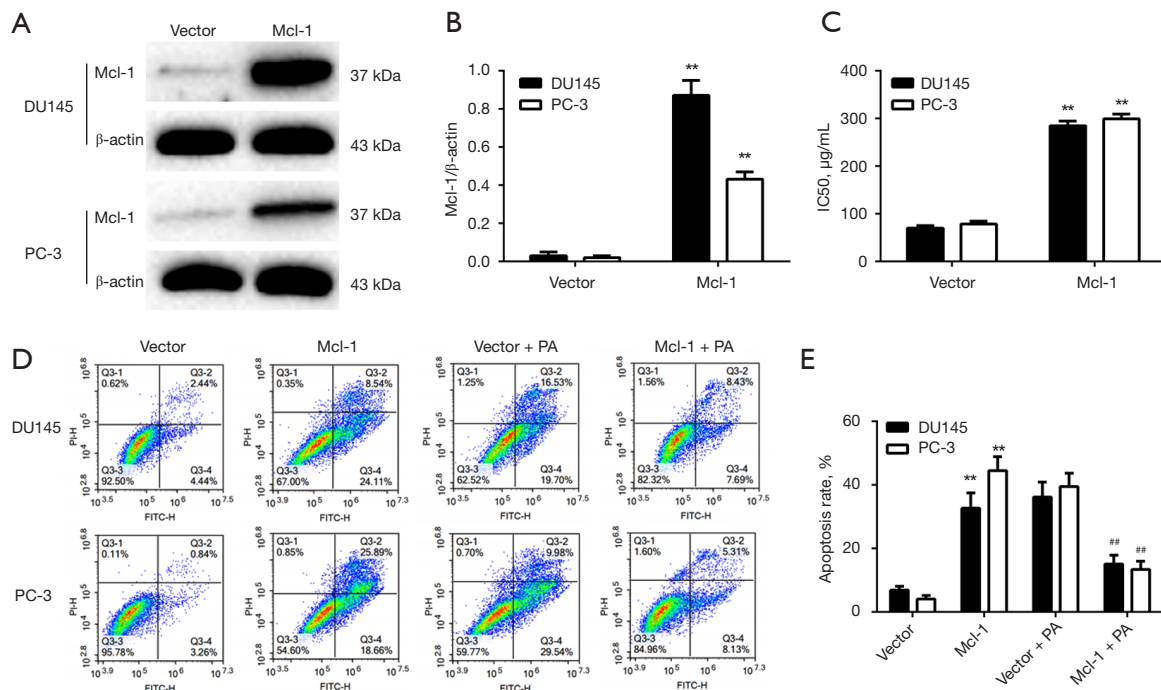


**Figure 5** Mcl-1 overexpression protects human CRPC cells from PA-induced apoptosis. (A) DU145 and PC-3 cells. After the transfection of Mcl-1 expression plasmid or vector for 48 h, Western blot was used to analyze the Mcl-1 protein levels. (B) Mcl-1 relative to  $\beta$ -actin expression. (C) After the DU145 and PC-3 cells were transfected with Mcl-1 expression plasmid or vector for 48 h, the IC<sub>50</sub> of the cells was calculated. The results are expressed as the mean  $\pm$  SD. Compared to the vector group, \*\*,  $P < 0.01$ . (D) After the DU145 and PC-3 cells were transfected with Mcl-1 expression plasmid or vector and cultured with or without PA (75  $\mu$ g/mL) for 48 h, apoptosis was analyzed by flow cytometry. (E) Apoptosis rate. The results are expressed as the mean  $\pm$  SD. Compared to the corresponding group, \*\*,  $P < 0.01$ ; ##,  $P < 0.01$ . CRPC, castration-resistant prostate cancer; PA, patchouli alcohol; SD, standard deviation.

treatment significantly reduced the protein expression of Ki67, p-p65, and MMP-2 (see *Figure 6E*), and the TUNEL positive cells increased significantly (see *Figure 6F*), which was consistent with the *in-vitro* results. We further confirmed that the PA treatment activated caspase-3 activity in tumor tissues and reduced the expression of Mcl-1, suggesting that PA induced apoptosis in a mitochondrial apoptotic pathway-dependent manner (see *Figure 6E*). Thus, we found that PA significantly inhibited the growth of PC-3 xenograft tumors by regulating the NF- $\kappa$ B signaling pathway *in vivo* with sufficient safety.

## Discussion

CRPC is a heterogeneous disease with a variety of mechanisms that lead to treatment resistance and disease progression. Combined chemotherapy and other treatments can prolong progression-free survival; however, these treatments ultimately fail to effectively prevent disease

progression (19,20). Thus, the treatment of CRPC needs to be improved. The malignant progression and therapeutic resistance of PCa are closely related to the activation of the NF- $\kappa$ B signal (21). A study has shown that the activation of the NF- $\kappa$ B signaling in PCa cells transforms androgen-sensitive PCa cells into androgen-insensitive cells and is associated with therapeutic resistance (22). The combination of anti-androgen and NF- $\kappa$ B targeted therapy effectively inhibits the tumor growth of human CRPC xenotransplantation (23). Additionally, anti-apoptotic protein Mcl-1 is highly expressed in CRPC, which is an inhibitor of apoptosis in the development of various malignant tumors and an important factor in anti-apoptosis (24). Thus, we speculate that the inhibition of the NF- $\kappa$ B/Mcl-1 signaling pathway represents a potential therapeutic target for CRPC. In a previous study, we found that PA effectively inhibited the proliferation and induced the apoptosis of human PCa PC3 cells (25). In this study, the *in-vitro* and *in-vivo* experiments showed that PA had

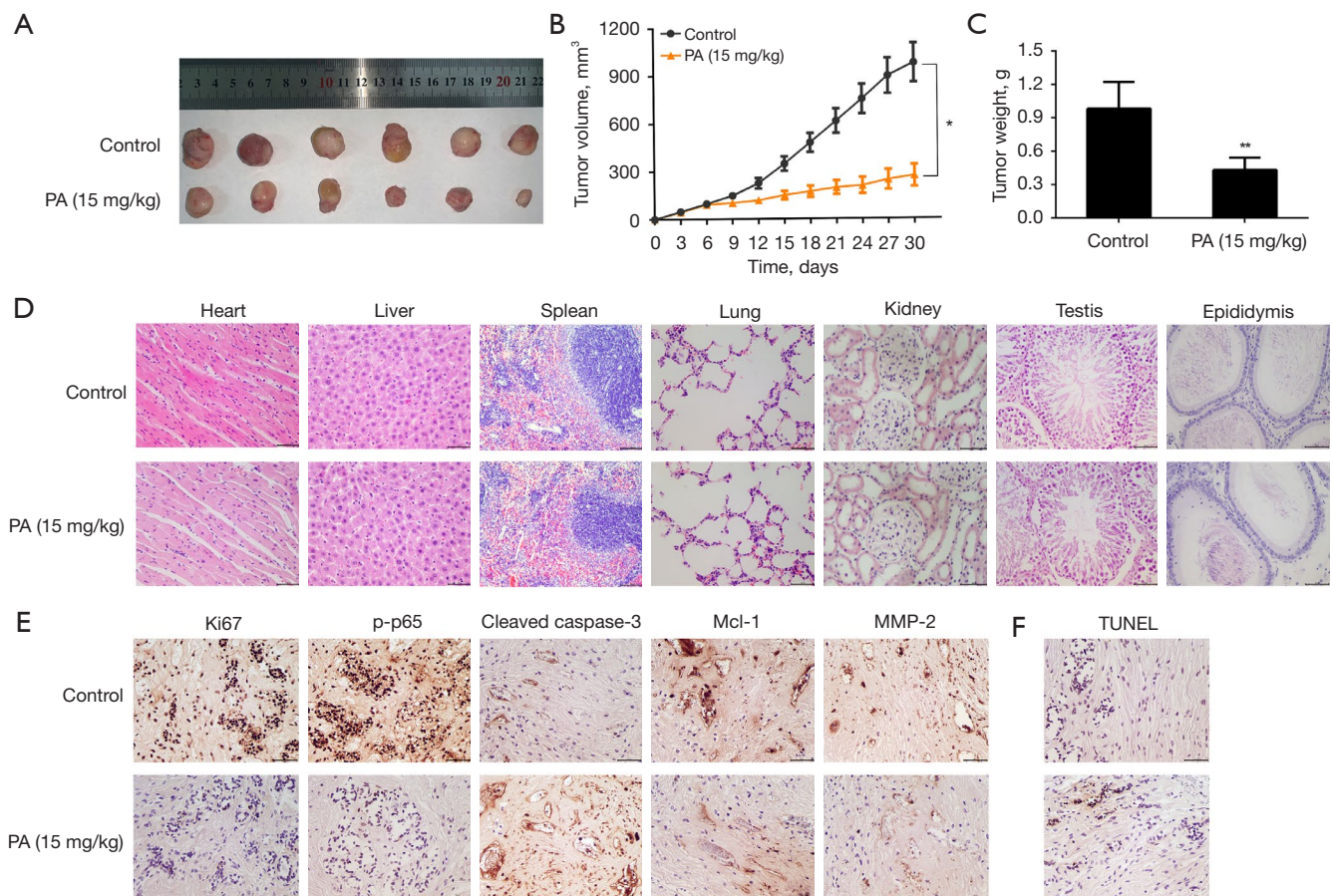


**Figure 6** PA inhibits PC-3 tumor growth *in vivo*. (A) Tumor images of mice in the control group and PA15 mg/kg dose group after 30 days. (B) Tumor volume measured every 3 days. (C) Tumor weight was weighed after 30 days. The results are expressed as the mean  $\pm$  SD. \*,  $P < 0.05$ ; \*\*,  $P < 0.01$ . (D) Histological analysis of normal tissues (heart, liver, spleen, lungs, and kidneys) and reproductive system related tissues (testis and epididymis) (H&E staining,  $\times 400$ ). (E) Immunohistochemistry was used to detect the expressions of Ki67, p-p65, cleaved caspase-3, Mcl-1, and MMP-2 in tumor tissues ( $\times 400$ ). (F) The TUNEL method ( $\times 400$ ) was used to detect apoptosis in tumor sections (apoptotic cells: brown). PA, patchouli alcohol; SD, standard deviation; H&E, hematoxylin and eosin; MMP, matrix metalloprotein; TUNEL, TdT-mediated dUTP nick-end labeling.

a significant inhibitory effect on the growth of CRPC subcutaneous xenografts, which significantly inhibited the proliferation and metastasis of CRPC cells and induced apoptosis.

PA as a natural drug has been reported to have good anti-tumor effects. Yang *et al.* (26) confirmed that PA inhibits tumor growth by regulating protein kinase B (Akt)/mammalian target of rapamycin (mTOR)-mediated autophagy in non-small cell lung cancer. In this study, we found that PA treatment resulted in the concentration- and time-dependent inhibition of CRPC cell viability, and further confirmed that PA inhibited the proliferation of CRPC cells *in vitro* by EdU staining and colony formation

assays. The antiproliferative mechanism is usually related to apoptosis (27). Apoptosis was observed by TUNEL staining. Annexin V/PI was measured by flow cytometry to verify PA-induced apoptosis. Mitochondrial dysfunction is the inducer of apoptosis (28), and its function is mainly regulated by Bcl-2 family apoptosis regulatory proteins. As anti-apoptotic and pro-apoptotic genes, Bax and Bcl-2 are considered essential to apoptosis regulation (29). Additionally, Bax forms apoptotic bodies, and caspase-3 is activated to induce apoptosis (30). We observed that CRPC cells treated with PA showed mitochondrial membrane potential loss, and the expressions of cleaved caspase-3, cleaved PARP, and Bax, and caspase-3 activity were



significantly upregulated, while the expression of Bcl-2 was inhibited.

At the same time, the addition of caspase inhibitors hindered the induction of apoptosis by PA. These findings indicate that the PA-mediated growth inhibition of CRPC cells involves the activation of the mitochondrial apoptosis pathway, which is consistent with the results of the *in-vivo* study. Notably, while PA can induce apoptosis, it has less toxic effects on normal organs. In this study, the H&E staining of the mouse testis and epididymis showed no significant damage except for the main organs. Additionally, the *in-vivo* and *in-vitro* experiments in this study showed that PA inhibited the migration, and invasion of the CRPC cells. More importantly, after PA treatment, the expressions of MMP-2, MMP-7, MMP-9, VEGF, and N-cadherin were downregulated, the expression of E-cadherin was upregulated. A study has shown that EMT processes can promote invasion and metastasis of tumor cells through intercellular connection and cell polarity (31). The characteristic manifestation of EMT is mainly reduced by epithelial cells such as E-Cadherin, and an increase in phenotype-specific protein of N-Cadherin equivalent cells (31). We further demonstrated that PA inhibits the invasion and migration of CRPC cells by inhibiting EMT activation.

Transcription factor NF- $\kappa$ B is the key medium for cell stress response and inflammation, and it has been proven that inhibiting the activity of NF- $\kappa$ B in cancer cell lines reduces the proliferation and metastasis of cells *in vivo* (32). Additionally, NF- $\kappa$ B plays an important role in regulating the mitochondrial apoptosis pathway (33). A study has shown that NF- $\kappa$ B/p65 is activated in the development and progression of PCa (28). The main mechanism of its activation involves the abnormal activation of inhibitor of NF- $\kappa$ B kinase (IKK), resulting in increased phosphorylation and the instability of the I $\kappa$ B protein (34). In this study, we treated DU145 and PC-3 cells with PA to inhibit the activation of the NF- $\kappa$ B pathway, and obtained the same results *in vivo*.

Additionally, the survival rate of the CRPC cells decreased and the apoptosis rate increased after transfection of p65 siRNA. PA treatment enhanced the proliferation inhibition and apoptosis promotion effect of p65 siRNA. It is speculated that apoptosis may be caused by reducing the phosphorylation of I $\kappa$ B $\alpha$  at Ser32/36, thereby limiting the nuclear translocation of NF- $\kappa$ B p65 and inhibiting DNA binding. Mcl-1 is a well-defined anti-apoptotic protein. There is evidence that Mcl-1 has nuclear localization

and is highly expressed in CRPC. Bao *et al.* (35) showed that  $\beta$ -elemenic acid inhibits the growth and induces the apoptosis of human CRPC cells by inhibiting the Janus kinase 2 (JAK2)/signal transducer and activator of transcription 3 (STAT3)/Mcl-1 and NF- $\kappa$ B signaling pathways. Reiner *et al.* (24) showed that some chemotherapy drugs targeting Mcl-1 induce DNA damage and lead to cell death, especially CRPC. A recent study showed that sildenafil enhances the sensitivity of CRPC cells to vincristine-induced mitochondrial apoptosis signal by downregulating Mcl-1 (36). In this study, the PA treatment significantly downregulated the expression of Mcl-1 in DU145 and PC-3 cells. Notably, the downregulation of Mcl-1 mediated by PA occurs at the transcriptional level, which is proven by the decrease of Mcl-1 transcripts, which is consistent with the fact that the phosphorylation of the NF- $\kappa$ B, a transcriptional activator of Mcl-1 is significantly inhibited by PA. The ChIP experiment directly showed that PA treatment inhibited the binding of NF- $\kappa$ B p65 to the Mcl-1 promoter. Thus, PA inhibited the transcription of Mcl-1 in the CRPC cells by inactivating NF- $\kappa$ B signal. Based on the above results, we speculated that PA-mediated apoptosis was partly achieved by inhibiting the expression of Mcl-1. In support of this hypothesis, the overexpression of Mcl-1 saved the growth inhibition of the CRPC cells induced by PA to some extent, and reversed the high apoptosis rate induced by PA.

## Conclusions

In summary, our study showed that PA has good therapeutic effects on CRPC and has minimal side effects. Additionally, the effect of inhibiting tumor growth and inducing apoptosis is related to the inhibition of the NF- $\kappa$ B/Mcl-1 pathway. Our findings provide novel insights and a theoretical basis for the study of PA resistance to CRPC.

## Acknowledgments

*Funding:* This work was supported by the Department of Science and Technology of Sichuan Province (No. 21ZDYF0466).

## Footnote

*Reporting Checklist:* The authors have completed the ARRIVE reporting checklist. Available at <https://tau.amegroups.com/article/view/10.21037/tau-22-220/rc>

*Data Sharing Statement:* Available at <https://tau.amegroups.com/article/view/10.21037/tau-22-220/dss>

*Conflicts of Interest:* All authors have completed the ICMJE uniform disclosure form (available at <https://tau.amegroups.com/article/view/10.21037/tau-22-220/coif>). All authors report that this work was supported by the Department of Science and Technology of Sichuan Province (No. 21ZDYF0466). The authors have no other conflicts of interest to declare.

*Ethical Statement:* The authors are accountable for all aspects of the work in ensuring that questions related to the accuracy or integrity of any part of the work are appropriately investigated and resolved. Animal experiments were performed under a project license (No. 2015-BL002) granted by ethics board of Hospital of Chengdu University of Traditional Chinese Medicine, in compliance with the guidelines of the National Institutes of Health (NIH) for the care and use of animals.

*Open Access Statement:* This is an Open Access article distributed in accordance with the Creative Commons Attribution-NonCommercial-NoDerivs 4.0 International License (CC BY-NC-ND 4.0), which permits the non-commercial replication and distribution of the article with the strict proviso that no changes or edits are made and the original work is properly cited (including links to both the formal publication through the relevant DOI and the license). See: <https://creativecommons.org/licenses/by-nc-nd/4.0/>.

## References

1. Ma L, He H, Jiang K, et al. FAM46C inhibits cell proliferation and cell cycle progression and promotes apoptosis through PTEN/AKT signaling pathway and is associated with chemosensitivity in prostate cancer. *Aging (Albany NY)* 2020;12:6352-69.
2. Zilli T, Dal Pra A, Kountouri M, et al. Prognostic value of biochemical response to neoadjuvant androgen deprivation before external beam radiotherapy for prostate cancer: A systematic review of the literature. *Cancer Treat Rev* 2016;46:35-41.
3. Berlin A, Fernández MI. Advances in the treatment of castration-resistant prostate cancer: emphasis in new hormonal therapies. *Rev Med Chil* 2015;143:223-36.
4. Lee DJ, Cha EK, Dubin JM, et al. Novel therapeutics for the management of castration-resistant prostate cancer (CRPC). *BJU Int* 2012;109:968-85.
5. Tian Y, Zhao L, Wang Y, et al. Berberine inhibits androgen synthesis by interaction with aldo-keto reductase 1C3 in 22Rv1 prostate cancer cells. *Asian J Androl* 2016;18:607-12.
6. Sánchez BG, Bort A, Mateos-Gómez PA, et al. Combination of the natural product capsaicin and docetaxel synergistically kills human prostate cancer cells through the metabolic regulator AMP-activated kinase. *Cancer Cell Int* 2019;19:54.
7. Zheng X, Jiang Z, Li X, et al. Screening, synthesis, crystal structure, and molecular basis of 6-amino-4-phenyl-1,4-dihydropyrano[2,3-c]pyrazole-5-carbonitriles as novel AKR1C3 inhibitors. *Bioorg Med Chem* 2018;26:5934-43.
8. Prelaj A, Rebuzzi SE, Buzzacchino F, et al. Radium-223 in patients with metastatic castration-resistant prostate cancer: Efficacy and safety in clinical practice. *Oncol Lett* 2019;17:1467-76.
9. Jeong JB, Choi J, Lou Z, et al. Patchouli alcohol, an essential oil of *Pogostemon cablin*, exhibits anti-tumorigenic activity in human colorectal cancer cells. *Int Immunopharmacol* 2013;16:184-90.
10. Zheng YF, Xie JH, Xu YF, et al. Gastroprotective effect and mechanism of patchouli alcohol against ethanol, indomethacin and stress-induced ulcer in rats. *Chem Biol Interact* 2014;222:27-36.
11. Yu XD, Xie JH, Wang YH, et al. Selective antibacterial activity of patchouli alcohol against *Helicobacter pylori* based on inhibition of urease. *Phytother Res* 2015;29:67-72.
12. Xie YC, Tang F. Protective effect of *Pogostemon cablin* on membrane fluidity of intestinal epithelia cell in ischemia/reperfusion rats after ischemia/reperfusion. *Zhongguo Zhong Xi Yi Jie He Za Zhi* 2009;29:639-41.
13. Lu X, Yang L, Lu C, et al. Molecular Role of EGFR-MAPK Pathway in Patchouli Alcohol-Induced Apoptosis and Cell Cycle Arrest on A549 Cells In Vitro and In Vivo. *Biomed Res Int* 2016;2016:4567580.
14. Song Y, Chang L, Wang X, et al. Regulatory Mechanism and Experimental Verification of Patchouli Alcohol on Gastric Cancer Cell Based on Network Pharmacology. *Front Oncol* 2021;11:711984.
15. Wang H, Guo M, Wei H, et al. Targeting MCL-1 in cancer: current status and perspectives. *J Hematol Oncol* 2021;14:67.
16. Booy EP, Henson ES, Gibson SB. Epidermal growth factor regulates Mcl-1 expression through the MAPK-Elk-1 signalling pathway contributing to cell survival in

- breast cancer. *Oncogene* 2011;30:2367-78.
17. Liu H, Zheng H, Duan Z, et al. LMP1-augmented kappa intron enhancer activity contributes to upregulation expression of Ig kappa light chain via NF-kappaB and AP-1 pathways in nasopharyngeal carcinoma cells. *Mol Cancer* 2009;8:92.
  18. National Research Council (US) Committee for the Update of the Guide for the Care and Use of Laboratory Animals. *Guide for the Care and Use of Laboratory Animals*. 8th ed. Washington (DC): National Academies Press (US); 2011.
  19. Thakur A, Vaishampayan U, Lum LG. Immunotherapy and immune evasion in prostate cancer. *Cancers (Basel)* 2013;5:569-90.
  20. Zhang M, Zhang Y, Song M, et al. Structure-Based Discovery and Optimization of Benzo[d]isoxazole Derivatives as Potent and Selective BET Inhibitors for Potential Treatment of Castration-Resistant Prostate Cancer (CRPC). *J Med Chem* 2018;61:3037-58.
  21. Khurana N, Sikka SC. Targeting Crosstalk between Nrf-2, NF-κB and Androgen Receptor Signaling in Prostate Cancer. *Cancers (Basel)* 2018;10:352.
  22. Montes M, MacKenzie L, McAllister MJ, et al. Determining the prognostic significance of IKKα in prostate cancer. *Prostate* 2020;80:1188-202.
  23. Jin R, Yamashita H, Yu X, et al. Inhibition of NF-kappa B signaling restores responsiveness of castrate-resistant prostate cancer cells to anti-androgen treatment by decreasing androgen receptor-variant expression. *Oncogene* 2015;34:3700-10.
  24. Reiner T, de Las Pozas A, Parrondo R, et al. Mcl-1 protects prostate cancer cells from cell death mediated by chemotherapy-induced DNA damage. *Oncoscience* 2015;2:703-15.
  25. Cai J, Peng C, Wan F, et al. The mechanism of patchouli oil inhibiting the proliferation and inducing the apoptosis of human prostate cancer cell line PC3. *Chinese Journal of Andrology* 2013;11:12-15,18.
  26. Yang L, Chen H, Li R, et al. Mufangji Decoction and Its Active Ingredient Patchouli Alcohol Inhibit Tumor Growth through Regulating Akt/mTOR-Mediated Autophagy in Non-small-Cell Lung Cancer. *Evid Based Complement Alternat Med* 2021;2021:2373865.
  27. Shi H, Tan B, Ji G, et al. Zedoary oil (Ezhu You) inhibits proliferation of AGS cells. *Chin Med* 2013;8:13.
  28. Chen X, Li S, Zeng Z, et al. Notch1 signalling inhibits apoptosis of human dental follicle stem cells via both the cytoplasmic mitochondrial pathway and nuclear transcription regulation. *Int J Biochem Cell Biol* 2017;82:18-27.
  29. Pang X, Zhang J, He X, et al. SPP1 Promotes Enzalutamide Resistance and Epithelial-Mesenchymal-Transition Activation in Castration-Resistant Prostate Cancer via PI3K/AKT and ERK1/2 Pathways. *Oxid Med Cell Longev* 2021;2021:5806602.
  30. Jin Z, Chenghao Y, Cheng P. Anticancer Effect of Tanshinones on Female Breast Cancer and Gynecological Cancer. *Front Pharmacol* 2022;12:824531.
  31. Kim SH, Choo GS, Yoo ES, et al. Silymarin induces inhibition of growth and apoptosis through modulation of the MAPK signaling pathway in AGS human gastric cancer cells. *Oncol Rep* 2019;42:1904-14.
  32. Shankar E, Zhang A, Franco D, et al. Betulinic Acid-Mediated Apoptosis in Human Prostate Cancer Cells Involves p53 and Nuclear Factor-Kappa B (NF- B) Pathways. *Molecules* 2017;22:264.
  33. Acuña UM, Mo S, Zi J, et al. Hapalindole H Induces Apoptosis as an Inhibitor of NF-κB and Affects the Intrinsic Mitochondrial Pathway in PC-3 Androgen-insensitive Prostate Cancer Cells. *Anticancer Res* 2018;38:3299-307.
  34. Nguyen DP, Li J, Yadav SS, et al. Recent insights into NF-κB signalling pathways and the link between inflammation and prostate cancer. *BJU Int* 2014;114:168-76.
  35. Bao X, Zhu J, Ren C, et al. β-elemnic acid inhibits growth and triggers apoptosis in human castration-resistant prostate cancer cells through the suppression of JAK2/STAT3/MCL-1 and NF-κB signal pathways. *Chem Biol Interact* 2021;342:109477.
  36. Hsu JL, Leu WJ, Hsu LC, et al. Phosphodiesterase Type 5 Inhibitors Synergize Vincristine in Killing Castration-Resistant Prostate Cancer Through Amplifying Mitotic Arrest Signaling. *Front Oncol* 2020;10:1274.
- (English Language Editor: L. Huleatt)

**Cite this article as:** Cai J, Zhao J, Gao P, Xia Y. Patchouli alcohol suppresses castration-resistant prostate cancer progression by inhibiting NF-κB signal pathways. *Transl Androl Urol* 2022;11(4):528-542. doi: 10.21037/tau-22-220